Lecture Notes: Salt Fingers **Ray Schmitt, Spring 05**

Stommel, Arons and Blanchard (1956) were considering the use of a pipe to the deep sea for use as a manometer to measure the pressure at the bottom of the ocean. If filled with bottom waters which are typically fresher than waters above, the height of water in the pipe would be higher than sea level and thus easily observed. However, they noted that heat flow through the pipe walls would allow a continuous flow of bottom water upward, creating a "salt fountain" driven by the density contrast between the fresh water in the pipe and the saltier surrounding waters, once the temperature contrasts had diffused. The flow would be perpetual so long as the temperature and salinity contrasts between surface and deep water were maintained by solar and atmospheric forcing, and the pipe was sufficiently conductive to heat.

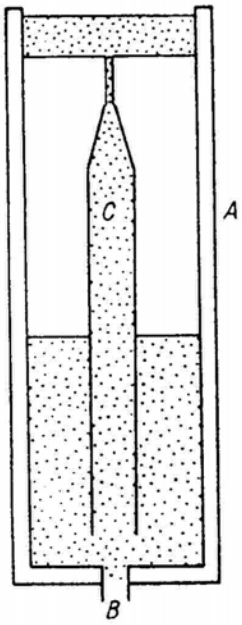

Fig. 1. Laboratory experiment to demonstrate the salt fountain, showing outside glass tube *A*, with hole in the bottom for filling *B*, and inner glass tube *C* to produce the fountain. The shading indicates the coloured water after the fountain has been in operation for some time.

Figure 1. The Salt Fountain
Experiment of Stommel, Arons and Blanchard (1956). They introduced the notion that potential energy of the salinity field could drive convective motions, but did not realize such motions could form on their own, due to the difference in the diffusivities of heat and salt.

A few years later, Stern (1960) opened up a new field of fluid dynamics now known as double–diffusive convection, by realizing that there was a two order of magnitude difference between the thermal conductivity of heat (1.4 x 10^{-7} m^2/s) in water and the diffusivity of dissolved salts (1 x 10^{-9} m^2/s). This difference allows the ocean to form its own pipes on a sufficiently small scale. The resulting "salt fingers" can be formed whenever warm salty water overlies cold fresh. An image of laboratory salt fingers is given in figure 2.

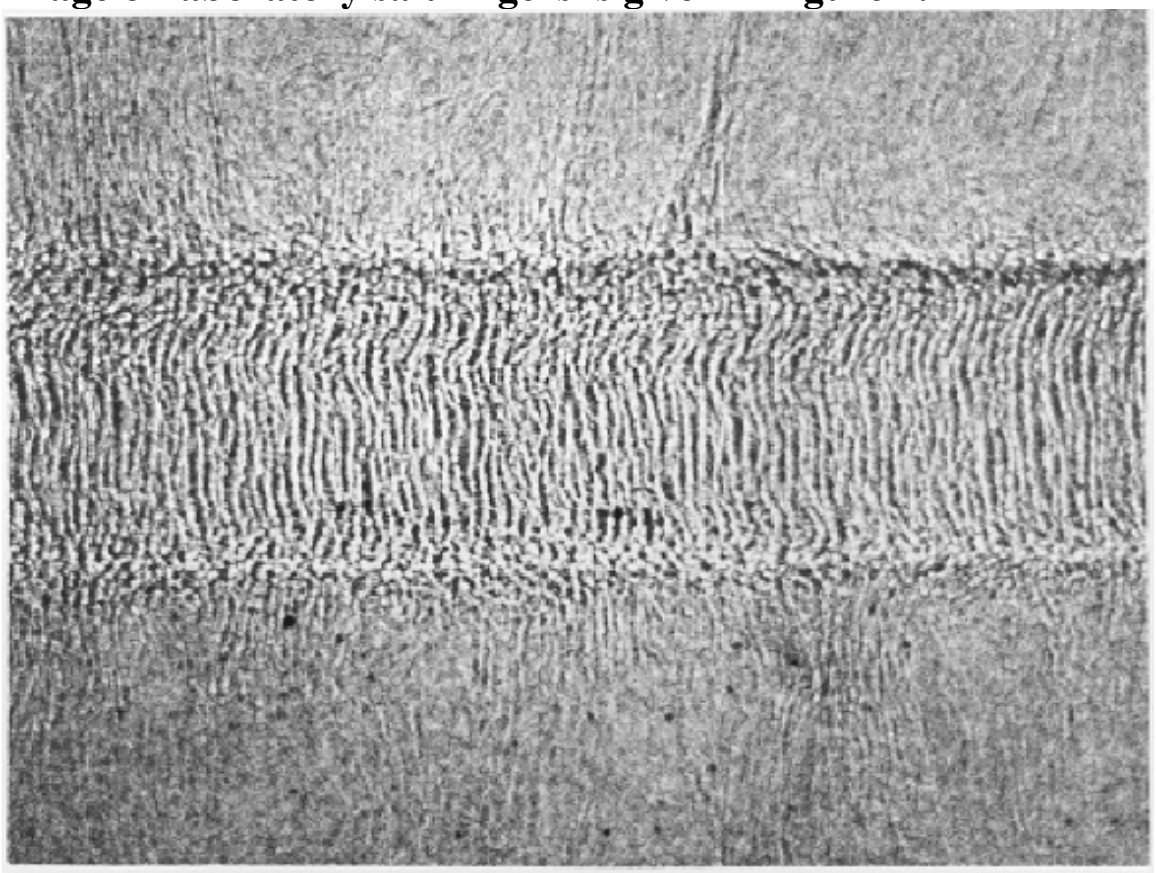

Figure 2. Laboratory shadowgraph of sugar-salt fingers at an interface between two mixed layers. The central fingering interface is 3 cm thick and the fingers about 1 mm wide. The shadowgraph is formed by projecting a collimated light beam through the fluid and imaging the pattern formed by index of refraction variations along the light path.

Any density affecting constituents with differing diffusivities can form a double-diffusive system, a common one for laboratory use is the sugar-salt system, where sugar diffuses at one third the rate of salt. In this case the sugar water represents the warm, salty water, the salt water the cold fresh.

The instability is readily understood by considering a parcel of water at an interface between warm salty water sitting above cold fresh water. Warm, salty parcels displaced downward into the cold fresh will lose heat by conduction but not much salt, so become cold salty and denser than adjacent water and continue to sink. Similarly, cold fresh parcels displaced upward get warmer but not much saltier and so become lighter that surrounding water and continue to rise. The finger instability occurs at a scale at which thermal conduction can effectively release the potential energy in the salt field, while not being overly damped by viscosity, or the diffusion of salt. Stern (1960) identified the scale of the fastest growing finger as:

$$l_F = 2\pi \left(\frac{g\alpha T_Z}{\nu \kappa_T} \right)^{-1/4}$$

This usually corresponds to a cell width ($l_F/2$) of 2-3 cm for oceanic conditions, but can be considerably smaller in the laboratory. Note that this scaling can be related to a Rayleigh number of order one and is defined entirely with local internal parameters, as no external length scale enters the expression. This independence from external length scales permits progress in understanding the properties of salt fingers by study of exact similarity solutions for salt fingers in an unbounded region with uniform T and S gradients.

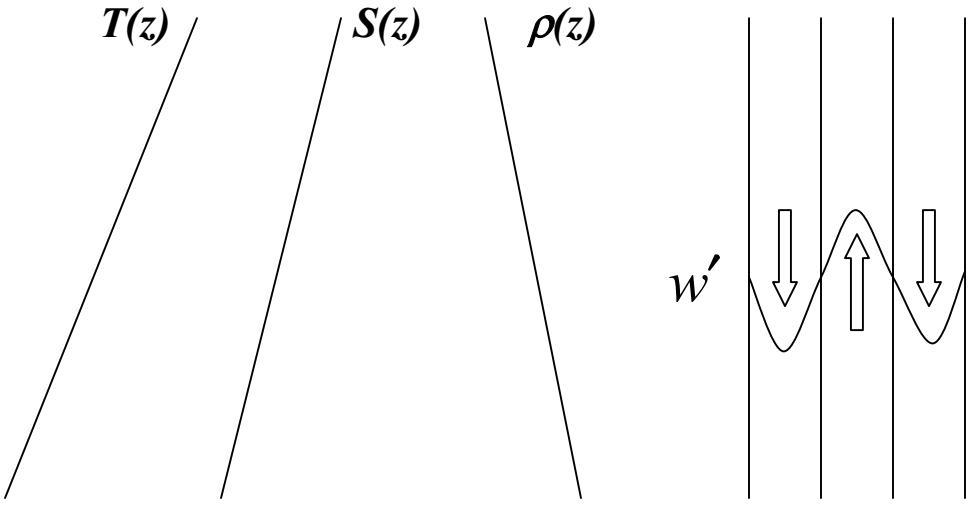

In the interior of such a linearly stratified ocean, it is possible to describe a field of purely vertical motions that remains valid at finite amplitude, because all the flows are parallel and the gradients of *T* and *S* are uniform. The heat and salt equations reduce to a balance between growth, vertical advection and horizontal diffusion (with ∇_2^2 = horizontal laplacian):

$$\frac{\partial T}{\partial t} + w\overline{T}_Z = \kappa_T \nabla_2^2 T$$

$$\frac{\partial S}{\partial t} + w\overline{S}_Z = \kappa_S \nabla_2^2 S \qquad \textbf{(1)}$$

The momentum balance is given by:

$$\frac{\partial w}{\partial t} = g(\alpha T - \beta S) + \nu \nabla_2^2 w$$

$$\text{where } \alpha \equiv -\frac{\partial \rho}{\rho \partial T}, \text{and } \beta \equiv \frac{\partial \rho}{\rho \partial S}.$$

We assume that a mean hydrostatic balance describes the pressure field and that no horizontal motions are associated with the initial growth of the vertical fingers.
The solutions to the foregoing equations are the mean fields:

$$\overline{T} = T_0 + (z - z_0)\overline{T}_Z$$

$$\overline{S} = S_0 + (z - z_0)\overline{S}_Z$$

and finger perturbations:

$$T', S', w' = (\hat{T}, \hat{S}, \hat{w}) \exp(\lambda t) \sin(kx) \sin(ky) .$$

Here λ is the exponential growthrate of the fingers, *k* is their horizontal wavenumber and the (^) represent "seed" amplitudes for the initial finger growth. Here we have used sin(*kx*)sin(*ky*) as a simple solution to the Helmholtz equation ($\nabla^2\phi - k^2\phi = 0$) that yields square packed fingers, a planform that is observed in the later stages of laboratory experiments.

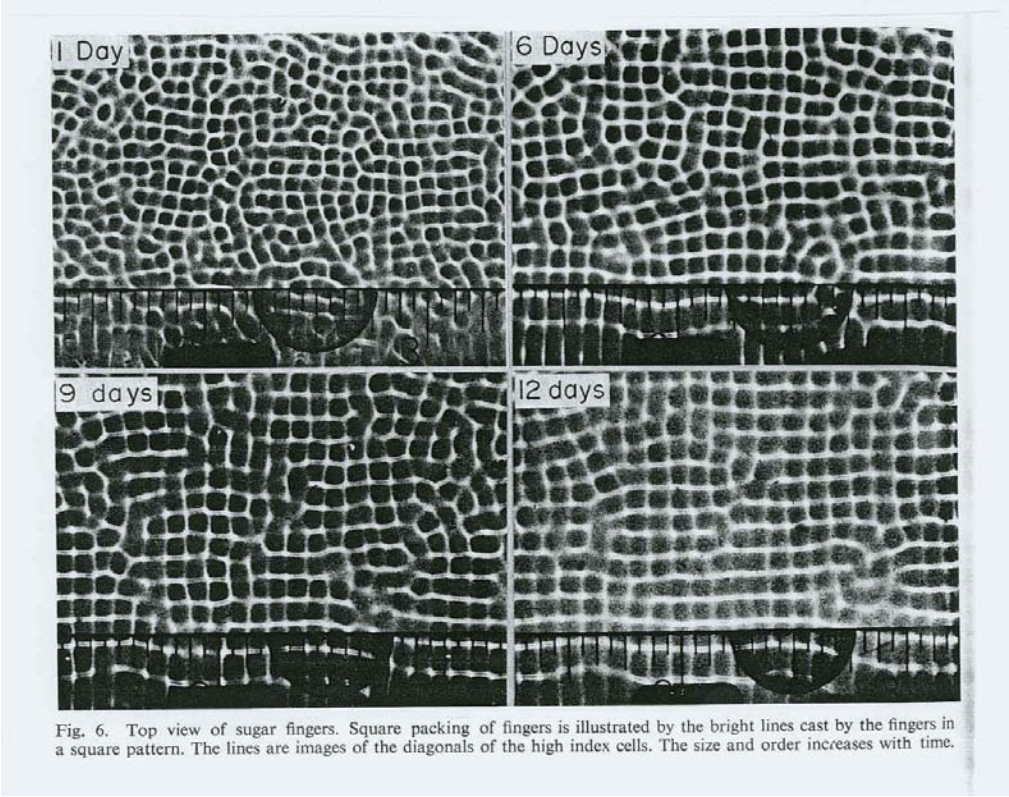

Fig. 6. Top view of sugar fingers. Square packing of fingers is illustrated by the bright lines cast by the fingers in a square pattern. The lines are images of the diagonals of the high index cells. The size and order increases with time.

Figure 4. Planform of laboratory fingers (Williams, 1975).

The growthrate depends on several non-dimensional parameters as well as the wavenumber and flux ratio of the fingers. There are two constants involving the diffusivities of heat salt and momentum, the Prandtl number, $Pr = \frac{\nu}{\kappa_T}$ **and the diffusivity ratio or Lewis number,** $Le = \frac{\kappa_T}{\kappa_S}$**. For seawater the Prandtl number is ~10 and the Lewis number ~100. The main environmental parameter is the density ratio R_ρ, given by:**

$$R_\rho \equiv \frac{\alpha T_Z}{\beta S_Z}$$

This expresses the degree to which the temperature gradient over-stabilizes the adverse salinity gradient; values much greater than one representing more stable water than those situations with near neutral stability (R_ρ=1), where fingers can grow most rapidly. For much of the subtropical thermocline, R_ρ tends to be near 2, indicating a strong propensity for salt fingering. The maximum density ratio at which fingers can grow is just the Lewis number (~100), since at that value the salinity gradient is too weak to overcome the damping effects of salt diffusion.

An important derived parameter for salt fingers is the ratio of the thermal buoyancy flux to the haline buoyancy flux. The flux ratio (γ) is defined as:

$$\gamma = \frac{\overline{w'\alpha T'}}{\overline{w'\beta S'}}$$

It can also be defined at any given wavenumber:

$$\gamma = \frac{\alpha T'(k)}{\beta S'(k)}$$

which is very useful for understanding salt finger dynamics.

That is, we expect a wide finger to retain a larger thermal anomaly due to reduced diffusion, while very narrow fingers would have a lower flux ratio due to the enhanced short circuiting of heat between up- and down-going fingers. Thus, a close connection between flux ratio and wave number is expected. We also note that energetics places an upward limit for the value of the flux ratio at 1.0, since no more buoyancy can be gained by the heat field than is extracted from the salt distribution. By setting the time derivative to zero in equation set (1), we can examine the properties of the "equilibrium finger", in which heat and salt diffusion just balance each other, and find that the lower limit of flux ratio at a given density ratio is just:

$$\gamma_{eq} = \frac{\kappa_S \alpha \overline{T}_Z}{\kappa_T \beta \overline{S}_Z} = \frac{R_\rho}{Le}$$

Thus, at low R_ρ a wide range of fingers can grow, but when $R_\rho \rightarrow Le$ only fingers with a flux ratio near one can exist. This limited range of allowable flux ratios and wavenumbers is the likely explanation for the increasing order displayed in finger planforms as experiments run down and one wavenumber comes to dominate the field (Figure 4). Strongly forced fingers at low density ratios are much more irregular in appearance, and numerical simulations display increasingly chaotic and turbulent appearing structures as $R_\rho \rightarrow 1$.

It is useful to examine these issues in a plot of flux ratio against density ratio (Figure 5). Values of flux ratio above the line represent growing fingers, those below are decaying fingers, with the equilibrium finger with $\lambda = 0$ $(\gamma = R_\rho / Le)$ line separating the two domains.

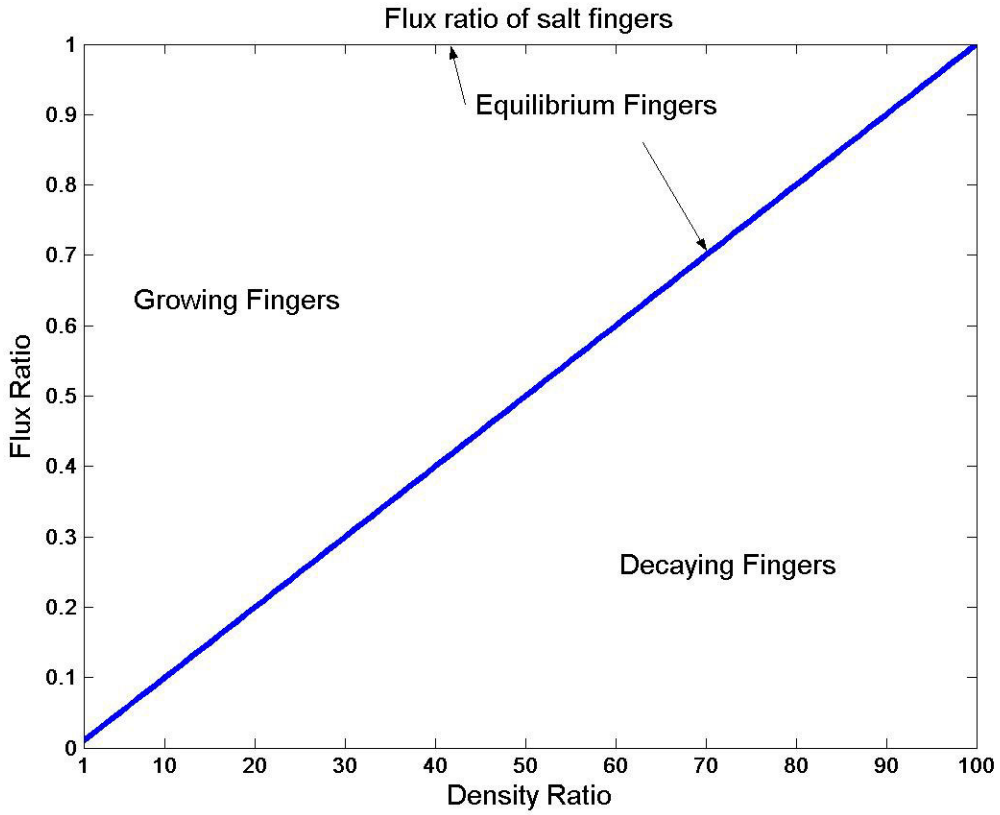

Figure 5. Flux ratio as a function of density ratio for heat-salt fingers. Energetics sets an upper limit of $\gamma = 1$, where heat and salt anomalies cancel and there is no density anomaly to drive the fingers. Salt diffusion sets a lower limit of $\gamma = R_\rho / Le$ where narrow fingers diffuse enough salt to yield zero growthrate. No fingers can form in a uniform gradient region for $R_\rho > Le \sim 100$.

Approximate solutions to Eq. (1) can be found in Stern (1976) and Kunze (1989), complete solutions are given in Schmitt (1979, 1983). These show that at low density ratios, the growth rate of the fastest growing finger varies as:

$$\lambda \simeq \left(\frac{\kappa_T}{\nu} \right)^{1/2} \left(g \alpha T_Z \right)^{1/2} \left[1 - (1 - R_\rho^{-1})^{1/2} \right]$$

This expression can also be cast in terms of the local buoyancy frequency (*N*) as:

$$\lambda \simeq \left(\frac{\kappa_T}{\nu}\right)^{1/2} N\left[(1-R_\rho^{-1})^{-1/2}-1\right]$$

where the relation $N=[\frac{-g\rho_Z}{\rho}]^{1/2}=[g(\alpha T_Z-\beta S_Z)]^{1/2}$ **has been used. Figure 6 displays this dependence on density ratio.**

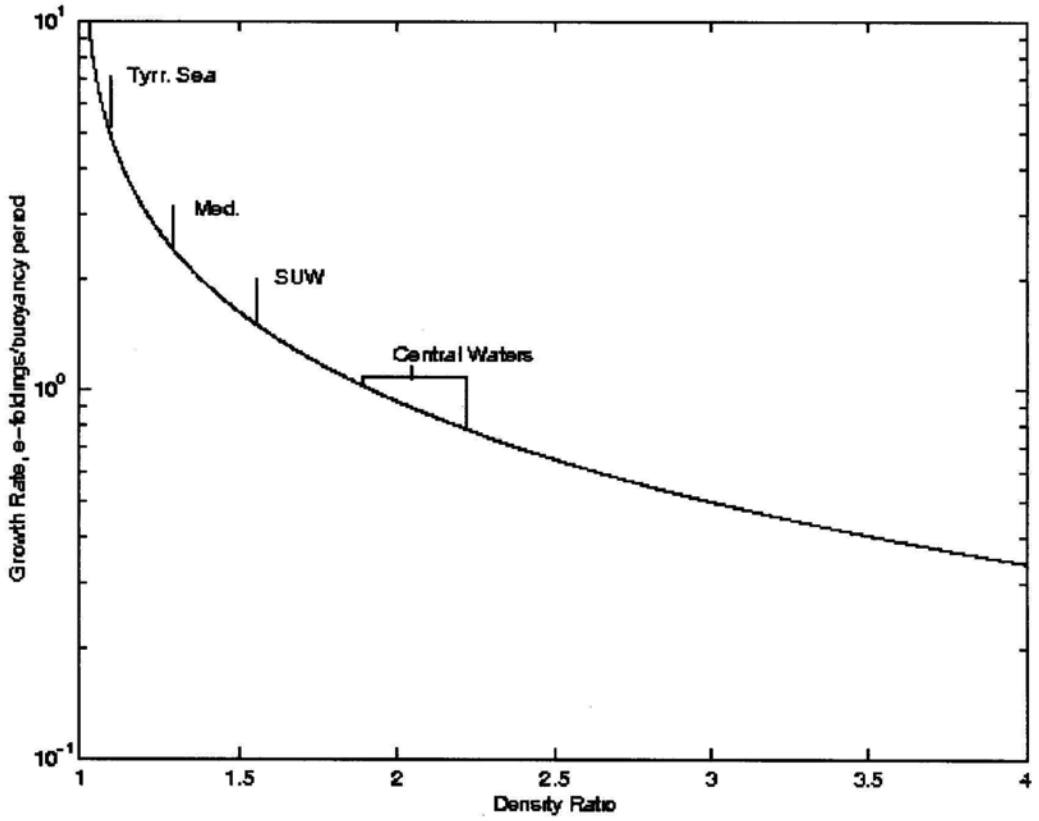

Figure 6. The growthrate of salt fingers for 1< R_ρ <4 with typical values of certain water masses noted. The growthrate has been scaled with the buoyancy period and is expressed in "e-foldings per buoyancy period". Fingers e-fold in amplitude in one buoyancy period in the central waters where R_ρ ~2.

The properties of the fastest growing finger are of special interest, as we expect those fingers to dominate the fluxes. In particular the observed flux ratios in both the heat-salt and salt-sugar systems is in good agreement with the flux ratio of the fastest growing finger (Figure 7). This is encouraging, given the large differences in Prandtl number and Lewis number.

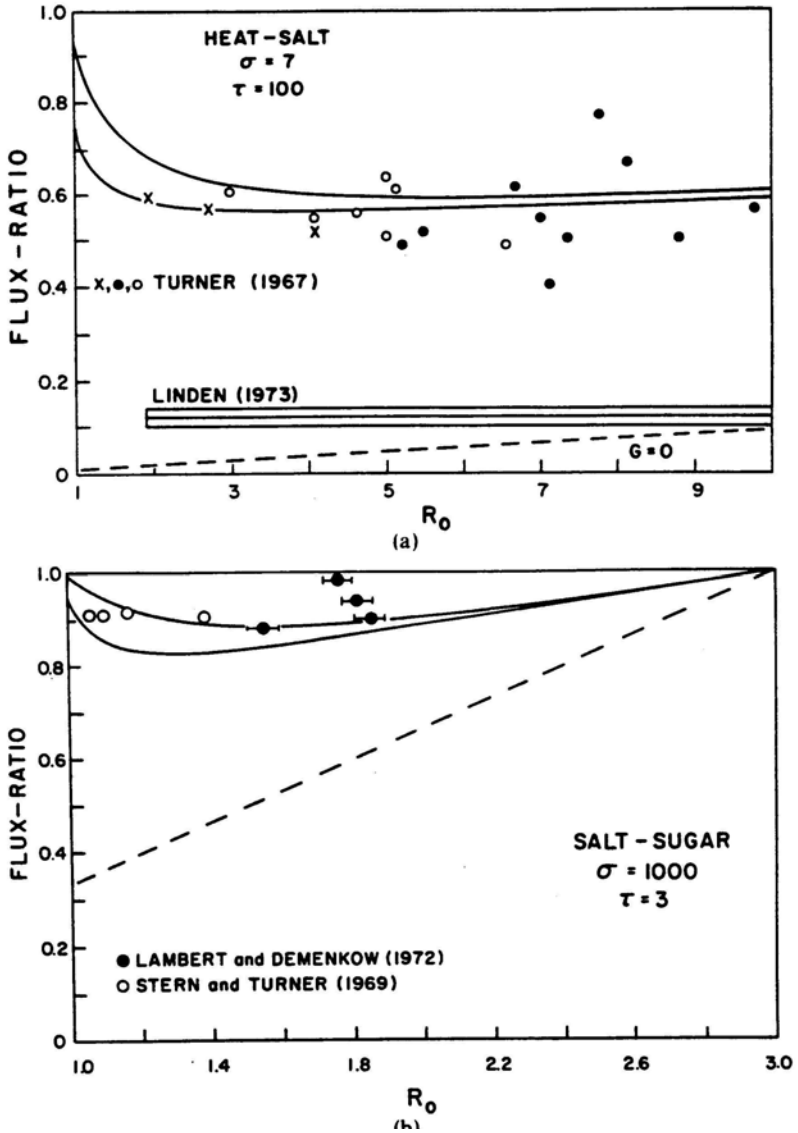

Figure 7. Flux ratio from laboratory data compared with the flux ratio of the fastest growing finger (solid curves) in the heat-salt and salt- sugar regimes. The equilibrium finger with λ=0 is shown as a dashed line. From Schmitt (1979).

The other parameter of interest is the horizontal wavenumber, which is closely related to the flux ratio as explained previously. A spectrum of growing fingers can be estimated, given a seed spectrum, by evaluation of the solutions to Eq (1). Figure 8 shows several such spectra evaluated after different growth times, for a typical central water density ratio of 2.

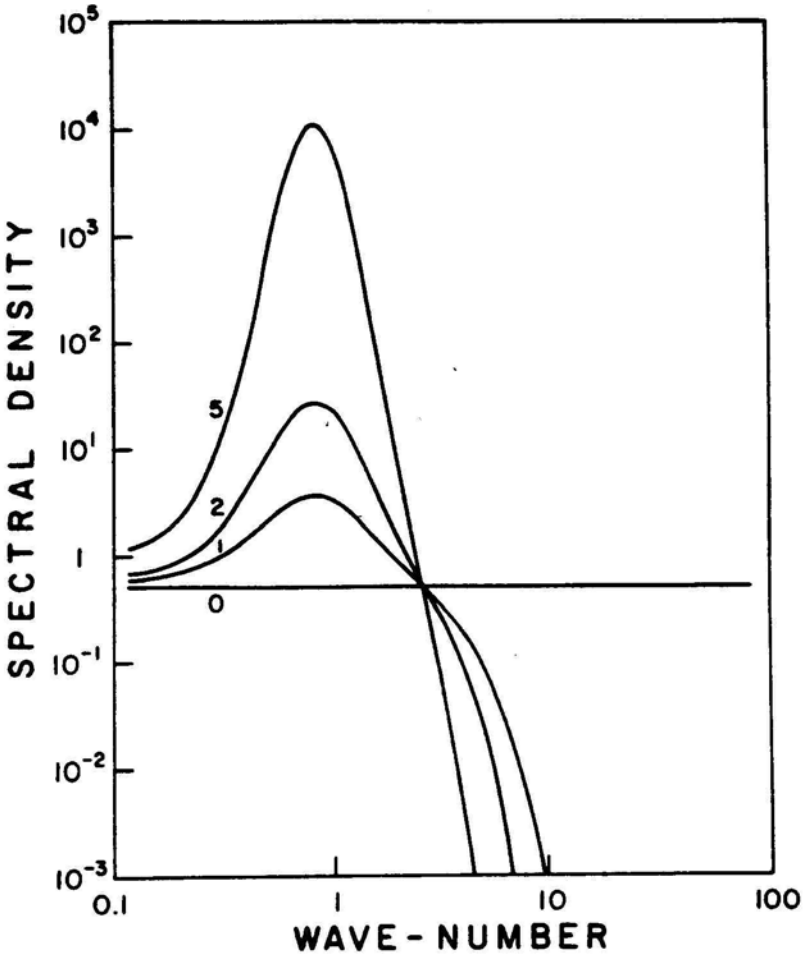

Figure 8. Horizontal wavenumber spectra (of temperature, salinity or vertical velocity) after 1, 2 and 5 buoyancy periods of growth from a "white noise" seed spectrum. The density ratio is 2 and the wavenumber scaling is $\left(g\alpha T_z / \nu\kappa_T\right)^{1/4}$.

Such theoretical spectra have shown success in predicting the location of the peak of the temperature gradient spectra in horizontal microstructure tows in a number of studies. One such is shown in Figure 9 below .

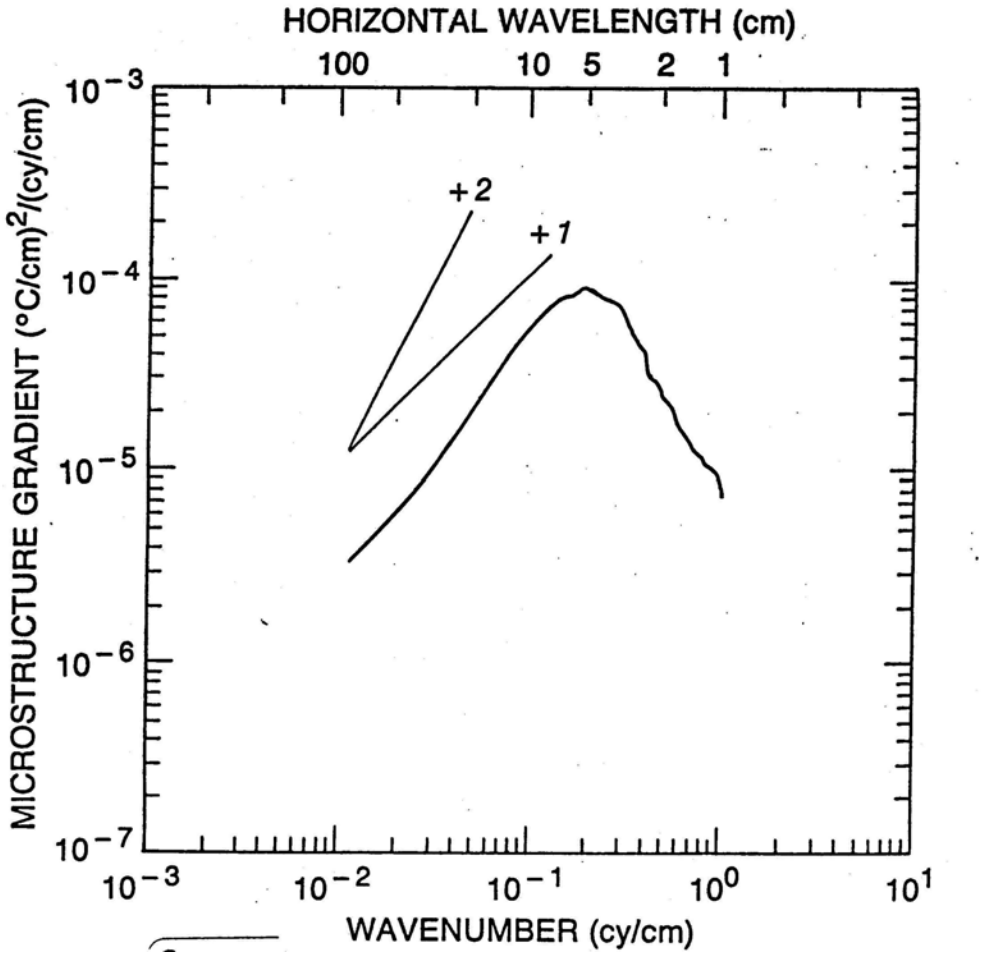

Figure 9. Horizontal wave number spectrum of temperature gradient for salt fingers observed at an interface between two mixed layers in the tropical Atlantic thermohaline staircase. The similarity theory predicts the fastest growing finger to be at 5 cm wavelength where the peak of the spectrum is observed. From Marmorino (1987).

Thermohaline Staircases

One of the macroscale signatures of double diffusion is the formation of a series of mixed layers from an initially stratified fluid. That is, the vertical property profiles resemble a staircase, with thin, high gradient interfaces separating the thicker well mixed layers. An example from a laboratory experiment with salt-sugar fingers is shown in Figure 10.

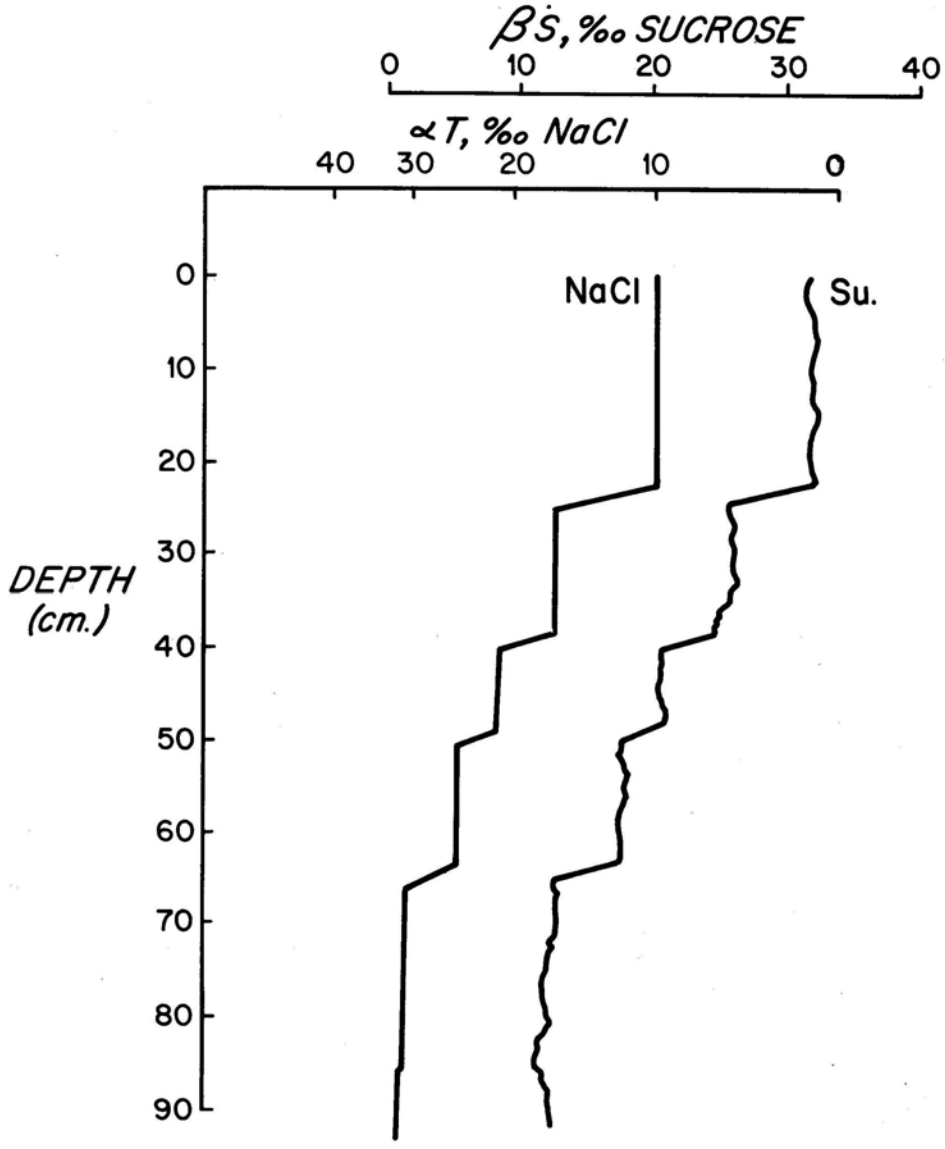

Figure 10. Thermohaline staircase formed from initially uniform gradients in the sugar-salt system.

Examples of a number of oceanic staircases are seen in Figure 11.

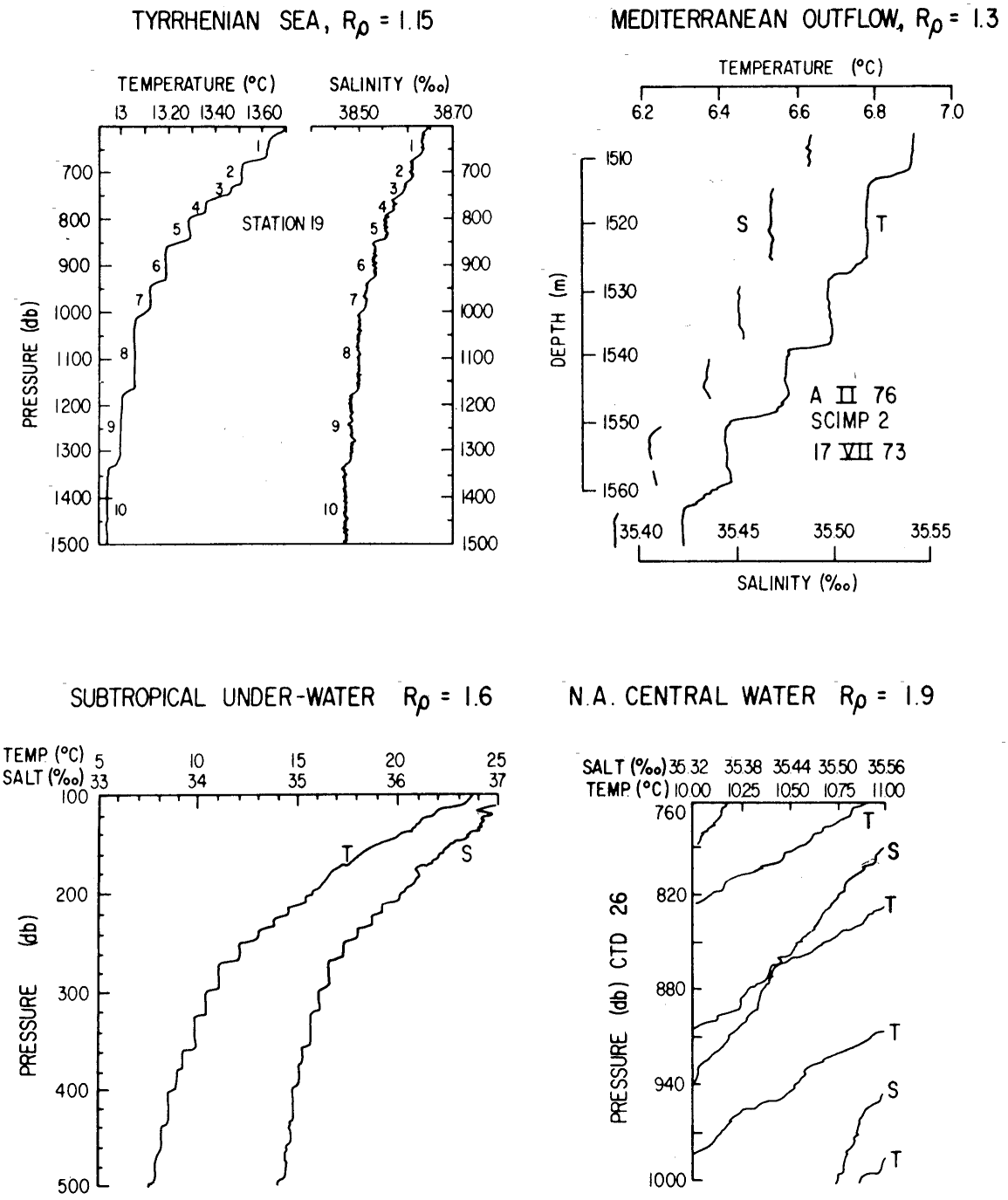

Figure 11. Salt finger staircases from some low density ratio water masses. Only irregular steps are observed at density ratios above ~1.7.

The mixed layers are maintained by stirring due to the net buoyancy flux through the interfaces, which because of the stronger gradients, harbor stronger finger fluxes than would occur in a uniform gradient. This provides one rationale for the existence of staircases. That is while the transports of heat and salt are down their respective gradients, the net transport of density is against its gradient. Thus, an initial density gradient becomes stronger after experiencing fingers, because the salinity gradient has been relaxed more strongly than the temperature gradient. Therefore, random increases in density gradient can be intensified, at the expense of adjacent weaker gradients. Once established, a mixed layer is easily stirred by the unstable buoyancy flux provided by the intensified double-diffusive mixing occurring in the interfaces.

Other explanations for staircases have been proposed by noting the collective instability arising when finger fluxes are redirected by internal waves (Stern, 1969) and due to the flux convergences arising from variations in the flux ratio with density ratio (Radko, 2003). The more recent theory appears promising because a limit on the size of layers may also be invoked (Radko, 2005).

One observed feature of oceanic staircases that supports a double diffusive interpretation is a strikingly tight T-S correlation within layers that can be traced horizontally for hundreds of kilometers. The variations in temperature and salinity for the staircase of the tropical Atlantic cut across isopycnals with a lateral density ratio of $R_l = \alpha \nabla_l T / \beta \nabla_l S =$ **0.85. Figure 12 illustrates this phenomenon. If flow within the layers is modified by vertical flux convergences due to fingers in the adjacent interfaces, then the T-S evolution must have a slope less than that of an isopycnal (R_l=1). Due to the variation of the thermal expansion coefficient with**

temperature, it is elevated above the expected value of the flux ratio alone (McDougall, 1990).

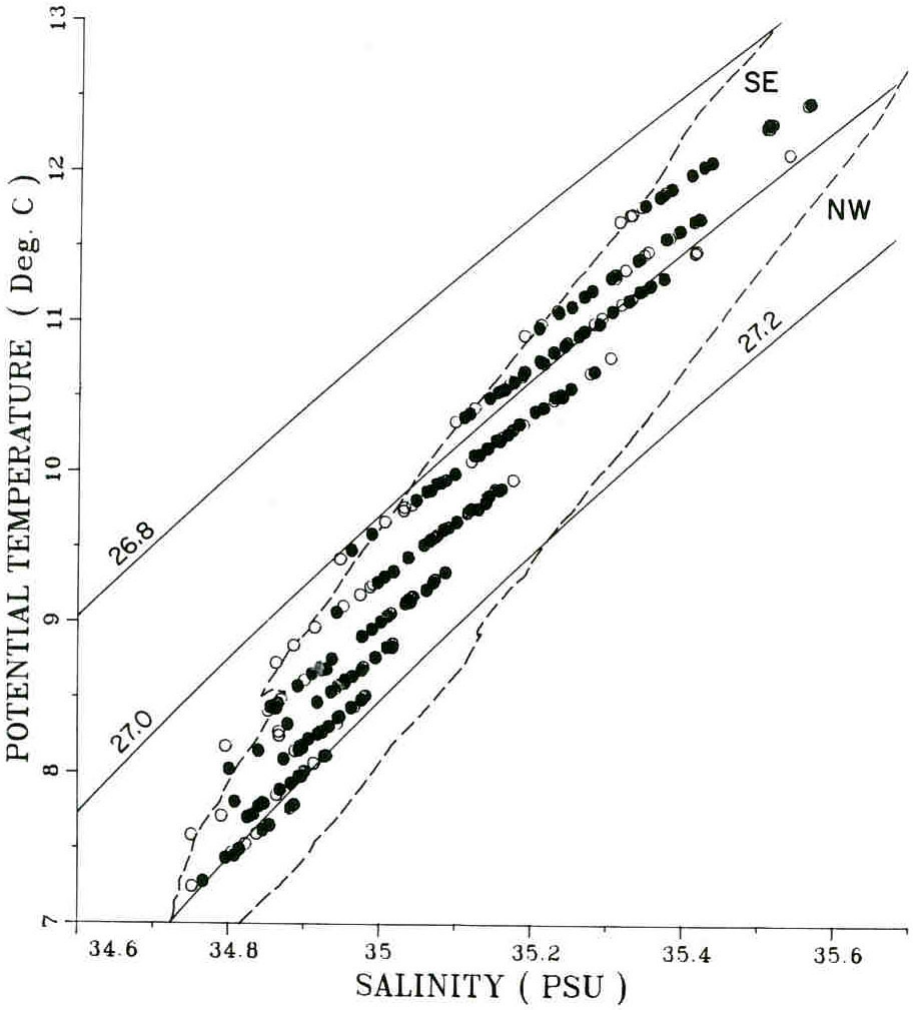

Figure 12. Variation of Temperature and Salinity in the mixed layers of the thermohaline staircase of the western tropical Atlantic. The black dots represent layers more than 10 m thick, the open circles layer between 5 and 10 meters thick. These trend lines cross potential density surfaces, indicating that a process with a heat/salt buoyancy flux ratio less than one is operating. Salt fingers are the only known mechanism that can explain this variation.

The layers of the tropical Atlantic occupy an area of ~1 million square kilometers east of the Caribbean and are occasionally found within the Caribbean itself (Figure 13).

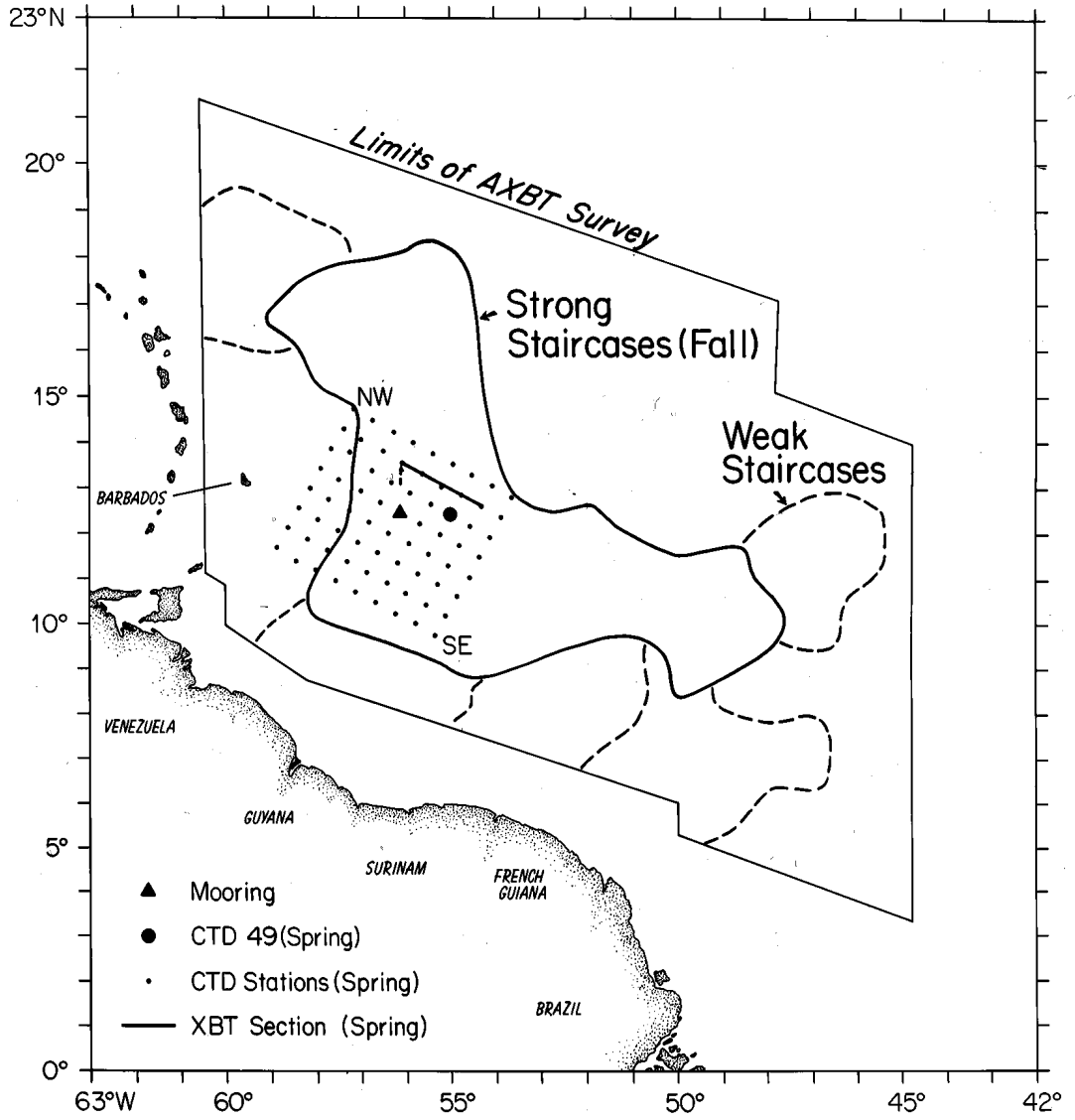

Figure 13. Area of thermohaline staircase in the western tropical Atlantic in Spring 1985 (from Schmitt et al, 1987). The outlined area was surveyed by air-deployed XBTs.

In order to quantify the mixing rate achieved in staircases, a tracer release experiment was recently performed in the tropical Atlantic. 175 Kg of the tracer sulfur hexaflouride (SF_6) were injected into a mid-staircase layer with a

temperature near 10°C. Nine months later a survey revealed the extent of vertical spread of the tracer (Figure 14).

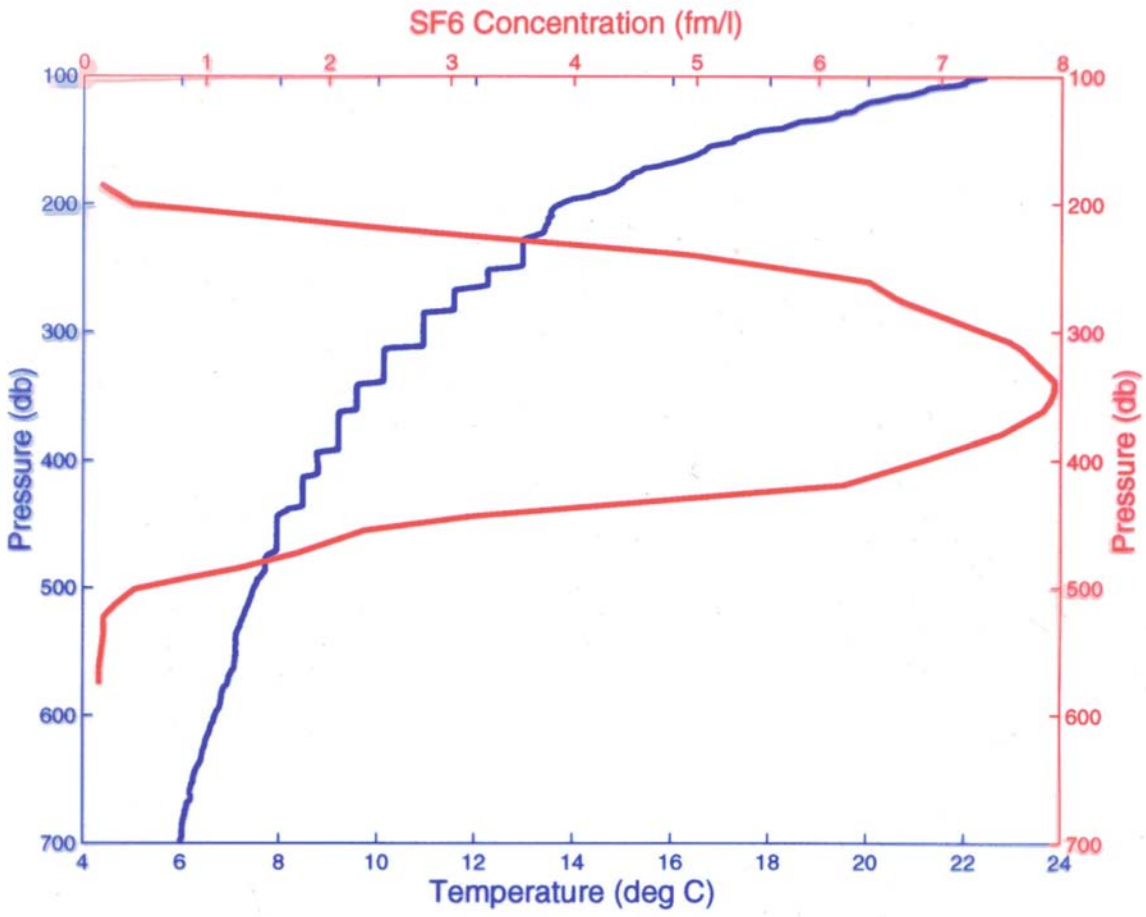

Figure 14. Vertical distribution of the tracer SF_6 (red) after nine months of mixing within a thermohaline staircase. The tracer was injected into the "10°C" layer in mid-staircase. (Schmitt et al 2005).

The increase of the vertical spread of tracer with time provides an estimate of the vertical diffusivity. If τ is the elapsed time between injection and sampling and σ the standard deviation of the tracer distribution about the mean depth, then the tracer diffusivity is just:

$$K_{SF_6} = \frac{\sigma^2}{2\tau}$$

For the tropical Atlantic staircase the tracer diffusivity turns out to be about 1 x 10^{-4} m^2/s. Because the tracer has nearly the same molecular diffusivity as salt, we expect the eddy diffusivity to be the same (the salt transport is advective in fingers). Microstructure observations in the staircase afford an opportunity to calibrate the models against the tracer dispersion data. Figure 15 shows the dissipation rate of thermal variance in a staircase along with the growthrate of salt fingers as calculated from the temperature and salinity profiles and the previously given formula.

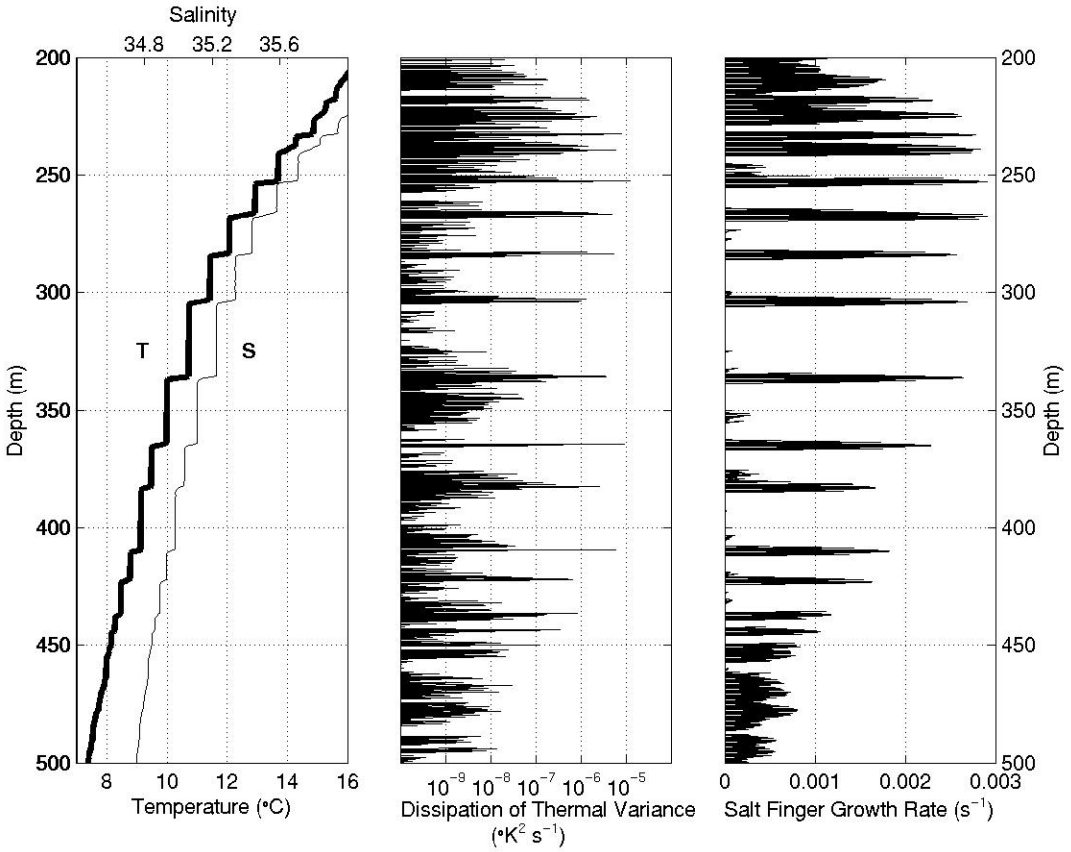

Figure 15. Profiles of temperature and salinity (left), dissipation rate of thermal variance (center) and salt finger growth rate (right), for an HRP station in the western tropical Atlantic.

The finger growthrate is correlated with the log of the dissipation rate, in a manner consistent with the "frozen growth" model previously applied to salt finger spectra. That

is, using the exact similarity solutions for fingers in locally uniform gradients, the finger amplitudes vary as:

$$T', S', w' \approx (\hat{T}, \hat{S}, \hat{w}) \exp(\lambda t) \sin(kx) \sin(ky)$$

The heat flux varies as:

$$\overline{w'T'} \approx \frac{1}{4} \hat{w}\hat{T} \exp(2\lambda t)$$

and the dissipation as:

$$\chi \approx \chi_0 \exp(2\lambda t)$$

$$\ln(\chi) \approx \ln(\chi_0) + 2\lambda t$$

This simple (but incomplete) model tends to fit the data with elapsed times of about 2-3 buoyancy periods.

The overall vertical eddy diffusivity for temperature appears to be one half as large as that for tracer and salt, based on the microstructure observations and the Osborn-Cox production – dissipation balance for thermal variance (Schmitt et al, 2005). This factor of two difference in the eddy diffusivities is to be expected for salt fingers. It is worth reiterating the production-dissipation balances predicted for turbulence and salt fingers:

Turbulence (Osborn, 1980; Osborn and Cox, 1972) (with flux Richardson number, $R_f = 0.17 \pm 0.03$**):**

$$K_\theta = K_S = K_\rho = \frac{R_f}{1 - R_f} \frac{\varepsilon}{N^2} \approx 0.2 \frac{\varepsilon}{N^2}$$

$$K_\theta = K_S = \frac{\chi_\theta}{2\overline{\theta_z}^2}$$

Salt fingers (McDougall, 1989) (with $R_\rho = 1.7$ and flux ratio $\gamma = 0.75$):

$$K_S = \frac{R_\rho - 1}{1-\gamma}\frac{\varepsilon}{N^2} \approx 2.8\frac{\varepsilon}{N^2}$$

$$K_S = \frac{R_\rho}{\gamma}\frac{\chi_\theta}{2\overline{\theta_z}^2} \approx 2.3K_\theta$$

$$K_\theta = \frac{\chi_\theta}{2\overline{\theta_z}^2}$$

These relationships show that fingers are much more "efficient" in mixing as compared to turbulence, as little of the energy derived from the salt field is dissipated, and more used to mix the temperature field. This accounts for the order of magnitude difference in the multiplier for ε/N^2.

We can also examine the behavior of the "scaled dissipation ratio" (Γ) introduced by Oakey (1989). It is defined as:

$$\Gamma = \frac{N^2\chi}{2\overline{\theta}_Z^2\varepsilon}$$

For turbulence we expect $\Gamma_T = \frac{R_f}{1-R_f} \simeq 0.2$, for fingers we predict $\Gamma_F = \left(\frac{R_\rho - 1}{R_\rho}\right)\left(\frac{\gamma}{1-\gamma}\right) \simeq 0.4 - 0.7$. St Laurent and Schmitt (1999) have examined the variation of Γ for oceanic microstructure in both double-diffusive and doubly-stable regimes by mapping its variation in a parameter space defined by the gradient Richardson number and the density ratio (R_ρ) and found elevated Γ in the low density ratio, high Richardson number regime. (Figure 16).

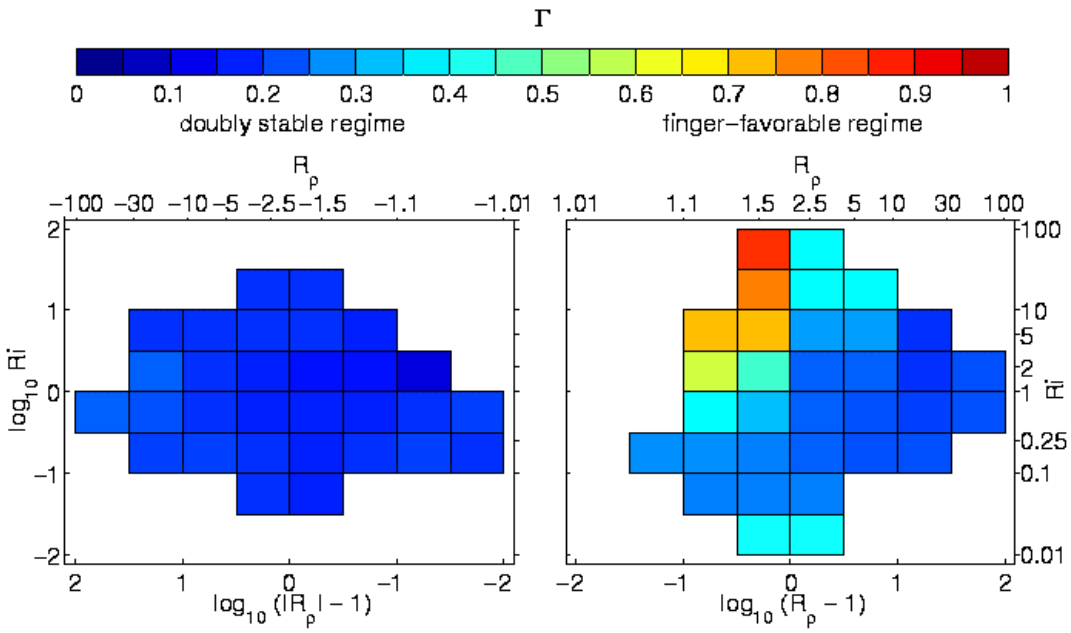

Figure 16. The scaled dissipation ratio as a function of Density Ratio and Richardson Number for microstructure observations with the High Resolution Profiler in both Atlantic (finger favorable) and Pacific (doubly stable) thermoclines. (St. Laurent and Schmitt, 1999)

In all of the doubly-stable regime the observed dissipation ratio is consistent with the expected value for turbulence. However, when the density ratio gets below two at higher Richardson numbers, an elevation of Γ is seen, consistent with salt fingering.

The evidence for salt finger activity at lower density ratios as seen in occurrence of microstructure and the appearance of thermohaline staircases, the near order of magnitude increase in tracer dispersion between the North Atlantic Tracer Release Experiment (St Laurent and Schmitt, 1999) (R_ρ~1.8) and the recent tropical Atlantic experiment (Schmitt et al, 2005) (R_ρ~1.6), as well as basic theory and laboratory experiments, suggests that oceanic mixing due to salt fingers is a strong function of the density ratio. Such a variation combined with

the greater transport of salt than heat, suggests a mechanism to directly affect the density ratio structure of the thermocline. There are two main effects: 1. the density ratio will tend to increase with time as the greater flux of salt than heat preferentially weakens the vertical salt gradient and, 2. any vertical variations in density ratio can produce flux convergences that tend to remove the density ratio anomaly. These can be explored with a density-ratio dependent mixing coefficient as in Schmitt (1981). The first effect is a likely explanation for the relative rarity of density ratios close to one outside of the surface layer (Ruddnick and Ferrari, 1999), it is most often close to two in the "central waters" of the subtropical gyres (Figure 17).

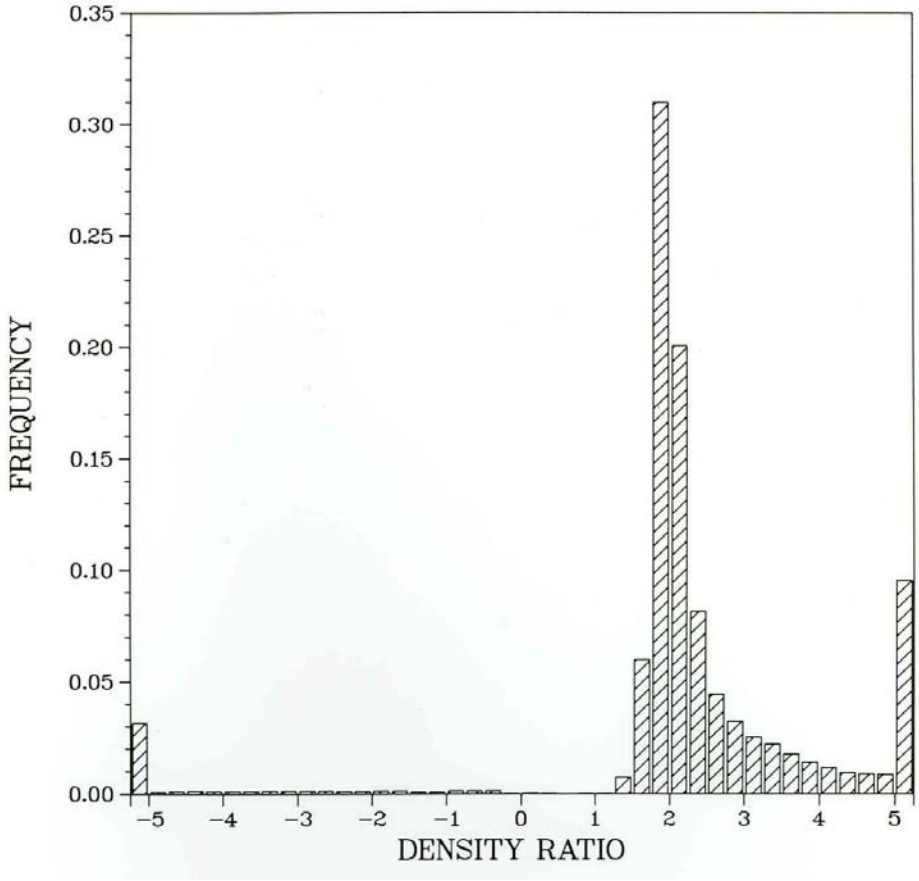

Figure 17. Histogram of R_ρ for the upper kilometer of the Atlantic at 24°N. R_ρ is computed over a 50 db vertical window from all CTD stations in a 24 N section (Schmitt, 1990).

The second effect is a powerful mechanism for producing "constant R_ρ" T-S correlations. That is, any anomaly in R_ρ is quickly removed by the flux convergences as illustrated with a one-dimensional model run in Figure 18.

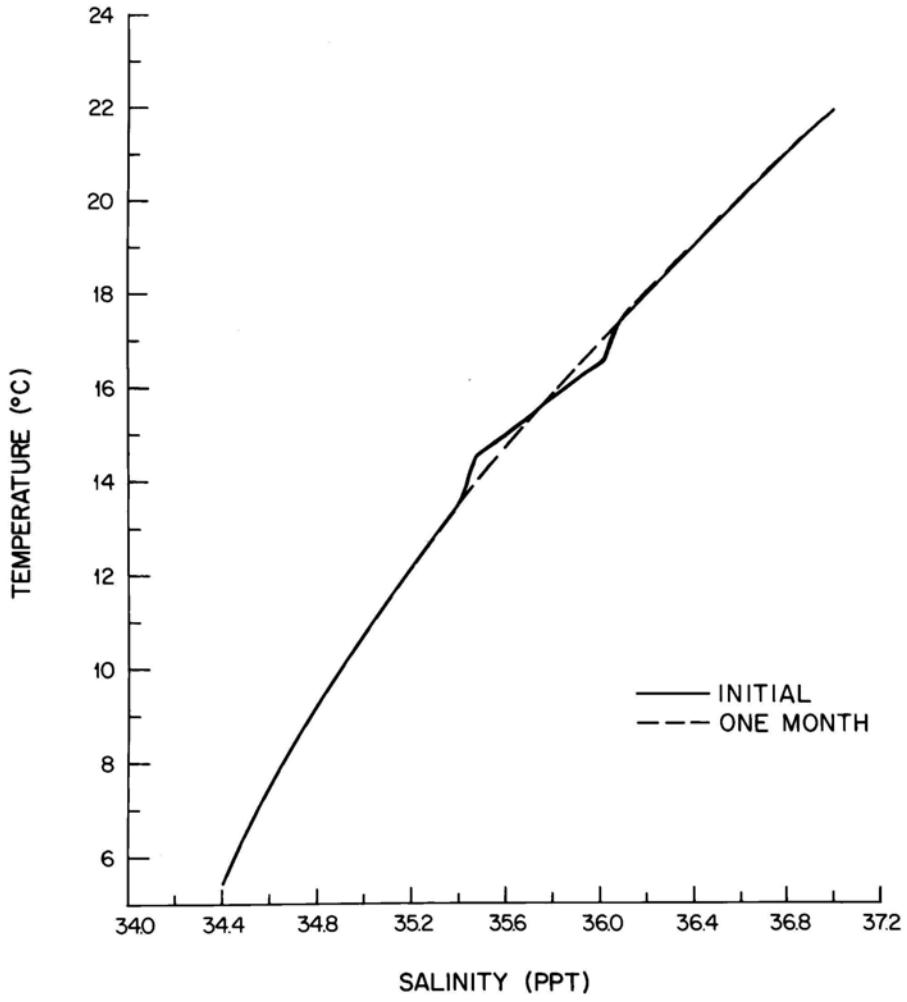

Figure 18. Temperature salinity diagram for the decay of a perturbation over one month, due to the density ratio dependent mixing rate predicted for salt fingering (Schmitt, 1981).

Thus, centimeter-scale salt fingers may be effective in influencing the large-scale mean structure of the thermocline.

Other fluid systems

Finally, since other geophysical regimes beyond the ocean may also support salt fingers, it is worth exploring their properties in a variety of fluid systems. The complete solutions of Schmitt (1979, 1983) permit such exploration, and a few results are illustrated in Figures 19 and 20.

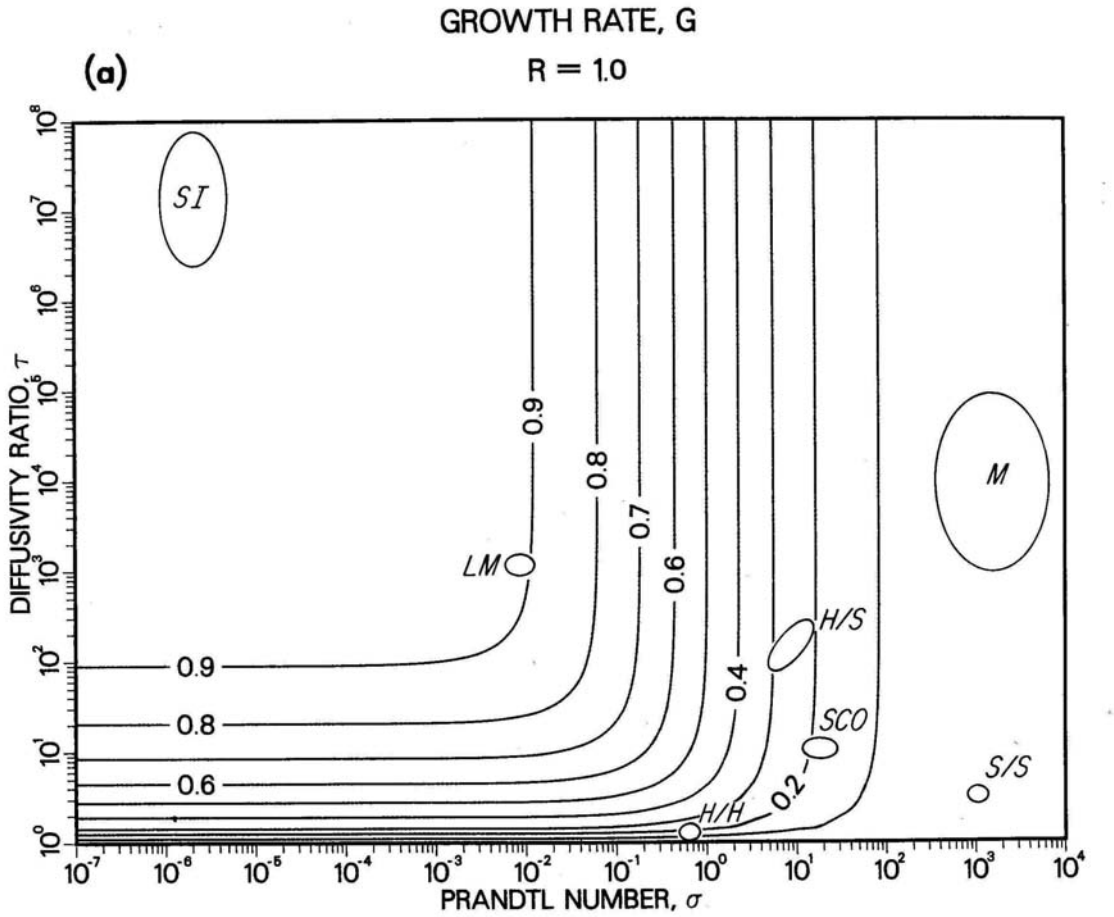

Figure 19. The growth rate of salt fingers at a density ratio of one for a wide range of Prandtl numbers and diffusivity ratios. Parameter ranges of various fluid systems are noted, these represent stellar interiors (SI), liquid metal (LM), magmas (M), oceanic heat/salt (H/S), salt/sugar (S/S), atmospheric heat/humidity (H/H), and semiconductor oxides (SCO). The viscous systems of sugar/salt and magmas are seen to be slow growing, while the low Prandtl number stellar interiors and liquid metal regimes have faster growth (Schmitt, 1983).

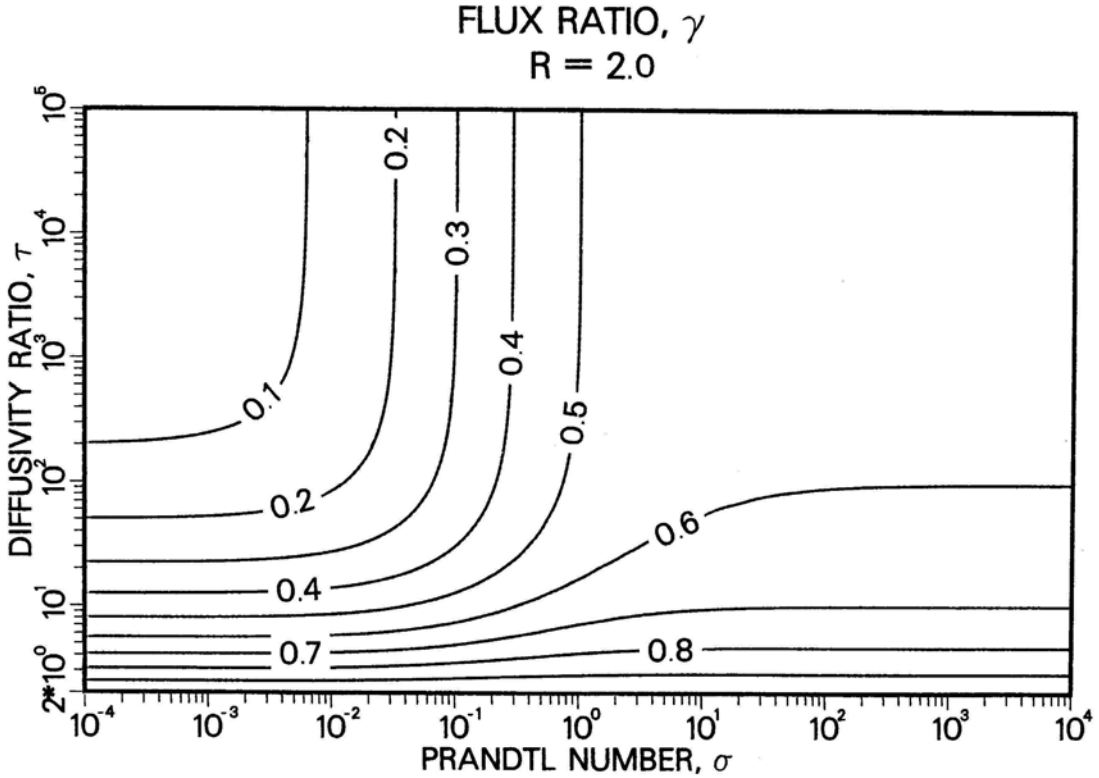

Figure 20. Flux ratio of the fastest growing finger at a density ratio of 2. The low Prandtl number systems have low flux ratio and the high Prandtl number systems have a flux ratio near 0.5, except where a low diffusivity ratio raises the flux ratio for all Prandtl numbers.

Some work has already been done on double diffusion in magmas and stars, and there is speculation that double-diffusive processes are active on other planets and moons in our solar system. Perhaps such calculations will prove useful in exploring and understanding the geophysical fluid dynamics of the atmospheres, oceans and interiors of other bodies in the solar system.

References:

Krishnamurty, R. 2003. Double-diffusive transport in laboratory thermohaline staircases. *J. Fluid Mechanics*, 483, 287-314.

Kunze, E., (1987). Limits on growing, finite length salt fingers: a Richardson number constraint. *Journal of Marine Research*, 45: 533-556.

Ledwell, J.R., Watson, A.J. & Law, C.S., (1993). Evidence for slow mixing across the pycnocline from an open-ocean tracer release experiment. *Nature*, 364: 701-703.

Lueck, R., (1987). Microstructure measurements in a thermohaline staircase. *Deep-Sea Research,* 34(10): 1677-1688.

Marmorino, G.O., (1991). Intrusions and diffusive interfaces in a salt-finger interface. *Deep-Sea Research*, 38 (11), 1431-1454.

Marmorino, G.O., Brown, W.K. & Morris, W.D., (1987). Two-dimensional temperature structure in the C-SALT thermohaline staircase. *Deep-Sea Research*, 23(10): 1667-1675.

McDougall, T.J., (1988). Some implications of ocean mixing for ocean modelling. In: J.Nihoul & B. Jamart (Editors), *Small-Scale Turbulence and Mixing in the Ocean.* Elsevier, New York, pp. 21-36.

McDougall, T.J., (1991). Interfacial advection in the thermohaline staircase east of Barbados. *Deep-Sea Research*, 38(3): 367-370.

Osborn, T. & Cox, C.S., (1972). Oceanic fine structure. *Geophysical Fluid Dynamics,* 3: 321-345.

Osborn, T.R., (1980). Estimates of the local rate of vertical diffusion from dissipation measurements. *Journal of Physical Oceanography*, 10: 83-89.

Radko, T., 2003: A mechanism for layer formation in a double-diffusive fluid. *J. Fluid Mech*., 497, 365-380.

Radko, T., 2005: What determines the thickness of layers in a thermohaline staircase? *J. Fluid Mech*., 523, 79-98.

Rudnick, D. L. & Ferrari, R., (1999). Compensation of horizontal temperature and salinity gradients in the ocean mixed layer. *Science*, 283:526-529.

Schmitt, R.W., (1979). The growth rate of super-critical salt fingers. *Deep-Sea Research,* 26A: 23-40.

Schmitt, Raymond W., 1983. The characteristics of salt fingers in a variety of fluid systems, including stellar interiors, liquid metals, oceans, and magmas. *Physics of Fluids*, 26(9), 2373–2377.

Schmitt, R.W., (1981). Form of the temperature-salinity relationship in the Central Water: evidence for double-diffusive mixing. *Journal of Physical Oceanography*, 11: 1015-1026.

Schmitt, R.W., (1987). The Caribbean Sheets And Layers Transects (C-SALT) Program. *EOS, Transactions of the American Geophysical Union*, 68(5): 57-60.

Schmitt, R.W., (1990). On the density ratio balance in the Central Water. *Journal of Physical Oceanography*, 20(6): 900-906.

Schmitt, R.W., (1994a). Double diffusion in oceanography. *Annual Review of Fluid Mechanics,* 26: 255-285.

Schmitt, R. W., (1994b). Triangular and asymmetric salt fingers. *Journal of Physical Oceanography*, 24(4): 855-860.

Schmitt, R.W., (1998). Double-diffusive convection: Its role in ocean mixing and parameterization schemes for large-scale modeling. In: E. Chassignet & J. Verron (Editors), *Ocean Modeling and Parameterization.* Kluwer Academic Publishers, 215-234.

Schmitt, R.W., (1999). Spice and the demon. *Science*, 283:498-499.

Schmitt, R., W., & Evans, D. L., (1978). An estimate of the vertical mixing due to salt fingers based on observations in the North Atlantic Central Water. *Journal of Geophysical Research*, 83: 2913-2919.

Schmitt, R. W., & Georgi, D. T. (1982). Finestructure and microstructure in the North Atlantic Current. *Journal of Marine Research*, Supplement to 40:659-705.

Schmitt, R.W., Perkins, H., Boyd, J. D. & Stalcup, M.C., (1987). C-SALT: an investigation of the thermohaline staircase in the western tropical North Atlantic. *Deep-Sea Research*, 34(10): 1697-1704.

Schmitt, R. W, J. R. Ledwell, E.T. Montgomery, K. Polzin and J. Toole, 2005. Enhanced diapycnal mixing by salt fingers in the thermocline of the tropical Atlantic. *Science*, in press.

Shen, C. & Schmitt, R.W., (1996). The wavenumber spectrum of salt fingers. In: A. Brandt & H. Fernando (Editors), *Double-Diffusive Convection*. AGU Geophysical Monograph, pp. 305-312.

St. Laurent, L. & Schmitt, R.W., (1999). The contribution of salt fingers to vertical mixing in the North Atlantic Tracer Release Experiment. *Journal of Physical Oceanography*, 29(7): 1404-1424.

Stern, M.E., (1960). The 'salt fountain' and thermohaline convection. *Tellus*, 12: 172-175.

Stern, M.E., 1969: Collective instability of salt fingers. *J. Fluid Mech.*, 35, 209-218.

Stern, M. E. and J. S. Turner, 1969. Salt fingers and convecting layers. *Deep-Sea Research*, 16, 497-511.

Turner, J. S., (1967). Salt fingers across a density interface. *Deep-Sea Research*, 14:599-611.

Turner, J. S., (1973). *Buoyancy effects in fluids*. Cambridge University Press, Cambridge, UK. 367 pp.

Williams, A.J., (1974). Salt fingers observed in the Mediterranean outflow. *Science*, 185: 941-943.

Williams, A.J., (1975). Images of Ocean Microstructure. *Deep-Sea Res.* 22, 811-829.